EFFECT OF SOUND ON LAMINAR-TURBULENT TRANSITION ON SWEPT WINGS

Sandrine Aubrun, Alain Seraudie, Daniel Biron and Daniel Arnal
ONERA, 2 avenue Edouard Belin, BP 4025, 31055 Toulouse Cedex 4, France

Keywords: *swept wing, transition, receptivity, sound, hot film and hot wire anemometry*

Abstract

The effect of sound on laminar-turbulent transition process is studied for 3D boundary layers governed by streamwise or crossflow instabilities. We quantify the shift upstream of the transition location versus sound level in both cases. We show that the effect of sound is characterized by a shortening of the transition length. Then, the comparison between linear stability theory results and experiments enables us to show that the excitation modify the initial amplitude of instabilities but not their amplification factor. Finally, we propose a relationship between the loss of N factor and sound level which is valid for streamwise or crossflow cases.

1 Introduction

The laminar-turbulent transition of a boundary layer is dependent on parameters such as velocity and pressure fluctuations of the external flow (turbulence intensity and acoustic level). In flight conditions, velocity fluctuations have low level but pressure fluctuations are not negligible and could be responsible of an early transition from laminar to turbulent flow. If the investigations dealing with the effect of sound on instabilities and on transition are common for 2D boundary layers[1, 2, 3], the rare works devoted to 3D cases seem to conclude that the sound has no effect on crossflow instabilities [4, 5]. In order to check this result, we have designed an experimental study with a swept ONERA D airfoil placed at different sweep angles and angles of attack. In this way, we can obtain different pressure distributions on the wing and so, different transition locations, due to different types of instabilities. The excitation is generated with a compressor driver. The upstream shift of the transition location due to sound have already been confirmed in our previous work [6] and the efficient frequency range was in agreement with frequency range of natural unstable waves. Now, the combination of information at the wall (hot films) and in the boundary layer (hot wire) allows us to explore how the sound acts on the transition process. To complete this study, we compare the amplification of unstable waves deduced from experimental results with computations based on linear stability theory. This calibration enables us to confirm the linearity of the receptivity. Finally, we propose a law of loss of amplification rate N versus the excitation level.

2 Experimental set-up

The model is a symmetric swept wing ONERA D type, its normal chord c is 0.35 m and its span is 2 m. The sweep angle is $\varphi = 60°$ and the tested angles of attack are $\alpha = -4°$ and $-8°$. The model is fixed in the middle of the test section (0.35*0.6 m^2) of an open low speed wind tunnel at ONERA Toulouse. Its circuit is carefully designed to reduce the contribution of freestream disturbances : the turbulence level $Tu = u'/Q_\infty$ is between 0.03% and 0.05%, and the acoustic noise $p'/\frac{1}{2}\rho Q_\infty{}^2$ is 0.3%. The reference velocity Q_∞ is between 50 and 80 m/s (associated chord Reynolds number Re_c between 1.2 10^6 and 1.9 10^6).

The acoustic excitation source is generated by a compressor driver JBL 2490H coupled with a specific horn (figure 1). We choose to produce as close as possible to the wing an acoustic plane wave propagating normally to the leading edge. In this way, we check that waves are subjected to a uniform deformation when they meet with the wing and so, they keep their plane characteristics downstream (at least on the first 30% chord) for frequency lower than 2500 Hz. The natural frequency response due to the loudspeaker coupled with the wind tunnel is not flat and so, some frequencies are favored. We build the generator signal (with the spectral analyzer Bruel & Kjaer 3550) to correct the frequential distribution of sound and make it flat in the area near the leading edge (location of the highest receptivity). This corrected signal is function of the angle of attack, of the sweep angle of the wing and of the flow velocity. The frequency range lies between 300 and 3000 Hz and the sound pressure level integrated on this frequency range can reach 130 dB.

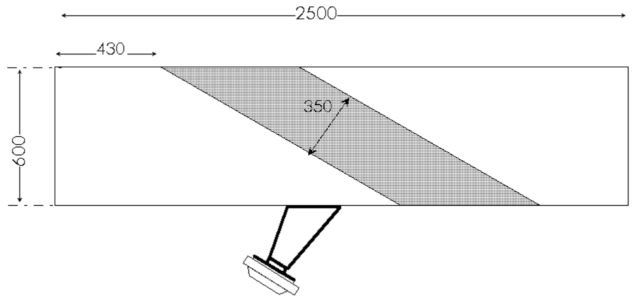

Figure 1: Swept wing in wind tunnel and compressor driver with specific acoustic horn.

To study the evolution of the transition location, 12 DANTEC hot film probes are stuck on the upper side of the model between 15 % and 80 % chord. The evolution of the root-mean-square level (of the output voltage of hot films) along the chord indicates the state of the boundary layer and the transition location. The rms level, particularly low in laminar flow, grows up, reaches a maximum in the intermittency region and comes down to the turbulent rms level. The latter stays higher than the laminar one. The transition criterion is based on the intersection between the line with the highest slope of velocity fluctuations and the laminar level. Nevertheless, some turbulent spots can appear upstream of this position.

In addition, some velocity measurements are performed with a single hot wire probe DANTEC type. They provide the mean profiles of velocity and turbulence intensity in the boundary layer.

The spectral analysis of hot films or hot wire signals allows us to identify unstable frequency ranges and effect of sound on spectral content of the boundary layer. Because these two devices give the same results about spectral content of the boundary layer, we will only present the spectral analysis of hot film signals.

3 Linear stability theory

We perform the stability calculations with the linear stability code CASTET. We use parallel flow approximation and we choose two methods to compute the streamwise integration of the amplification factor N :

$$N = \max_f \left[\ln\left(A(x)/A_0\right)\right] \qquad (1)$$

where A_0 is the amplitude of the initial perturbation on the neutral curve :

- the *envelope* method
- the *fixed* β^* method where β^* is a wave number in the crossflow direction.

Knowing the experimental transition location, the envelope method provides the frequency of the most unstable wave at transition. The *fixed* β^* method provides the couple (frequency - β^*) for the most unstable wave at transition. This wave is considered as responsible of transition. So, we can also deduce from stability computations, the theoretical amplification N factor and the direction of the wave number ψ at transition. The envelope method gives a frequency range of the most unstable instabilities in good agreement with experiments. On the other hand, the associated N factor is not really suitable to prediction of transition. In many cases, a given frequency is amplified first through the effect of crossflow instability ; downstream of the point of minimum pressure, it is then amplified through the effect of streamwise instability. And so, the N factor represents the cumulative contributions of crossflow and streamwise instabilities. This is not realistic. The *fixed* β^* method gives lower frequency ranges of unstable waves but it is well-adapted to prediction transition. Consequently, all our results based on theoretical N factor will be performed with the *fixed* β^* method.

4 Studied configurations

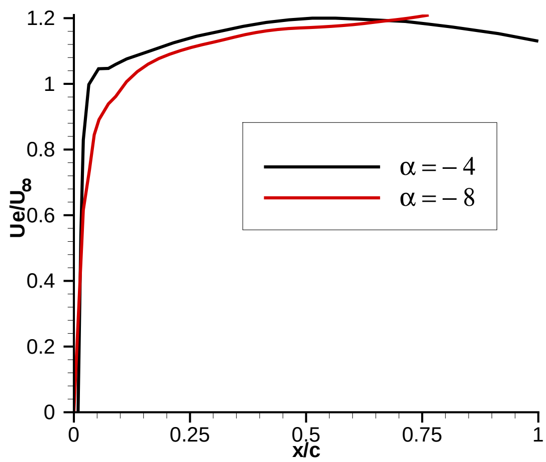

Figure 2: Velocity distributions on the model upper side.

In order to compare the effect of sound on transition due to streamwise or crossflow instabilities, we choose two configurations :

- The streamwise case is obtained with a sweep angle $\varphi = 60°$, an angle of attack $\alpha = -4°$ and a reference velocity $Q_\infty = 75 m/s$ ($Re_c = 1.8\ 10^6$). The free transition location is close to $x_t/c = 0.7$. The velocity distribution on the upper side of the model (fig. 2) shows that the velocity gradient is negative at transition. The linear stability theory (with envelope strategy) indicates that the direction of the wave vector of the most amplified mode at transition is $\psi = -10°$. The experimental frequency range of unstable waves deduced from hot wire measurement at transition in boundary layer ($x/c = 0.7$ and $y = 0.4mm$) is between 1200 and 3000 Hz which is in agreement with theory (fig. 3).

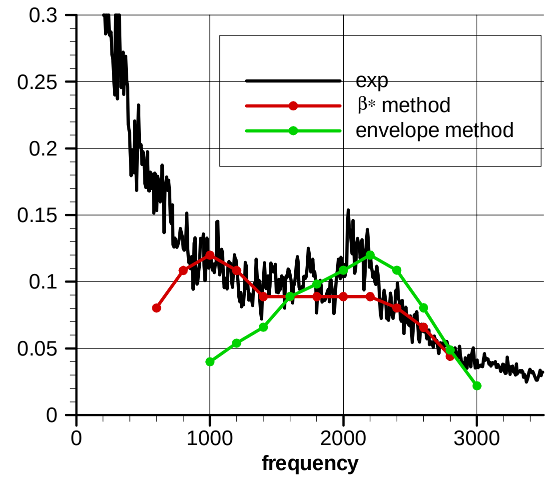

Figure 3: Comparison between experimental and theoretical spectral distribution of rms level at transition for streamwise case.

- The crossflow case is obtained with a sweep angle $\varphi = 60°$, an angle of attack $\alpha = -8°$ and a reference velocity $Q_\infty = 75 m/s$. The transition location is at $x_t/c = 0.25$. The velocity gradient is positive at transition. The linear stability theory indicates that $\psi = +65°$ at this point. The experimental frequency range of unstable travelling waves measured at transition ($x/c = 0.25$ and $y = 0.3mm$) is between 1200 and 3500 Hz which is in agreement with theory (fig. 4). In addition, the presence of stationary instabilities characterized by longitudinal vortices have been proved in [7].

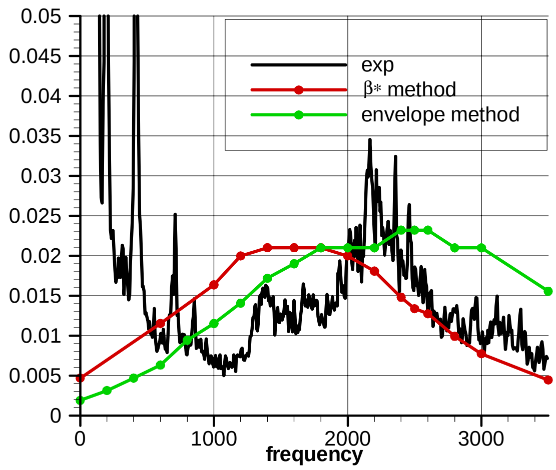

Figure 4 : Comparison between experimental and theoretical spectral distribution of rms level at transition for crossflow case.

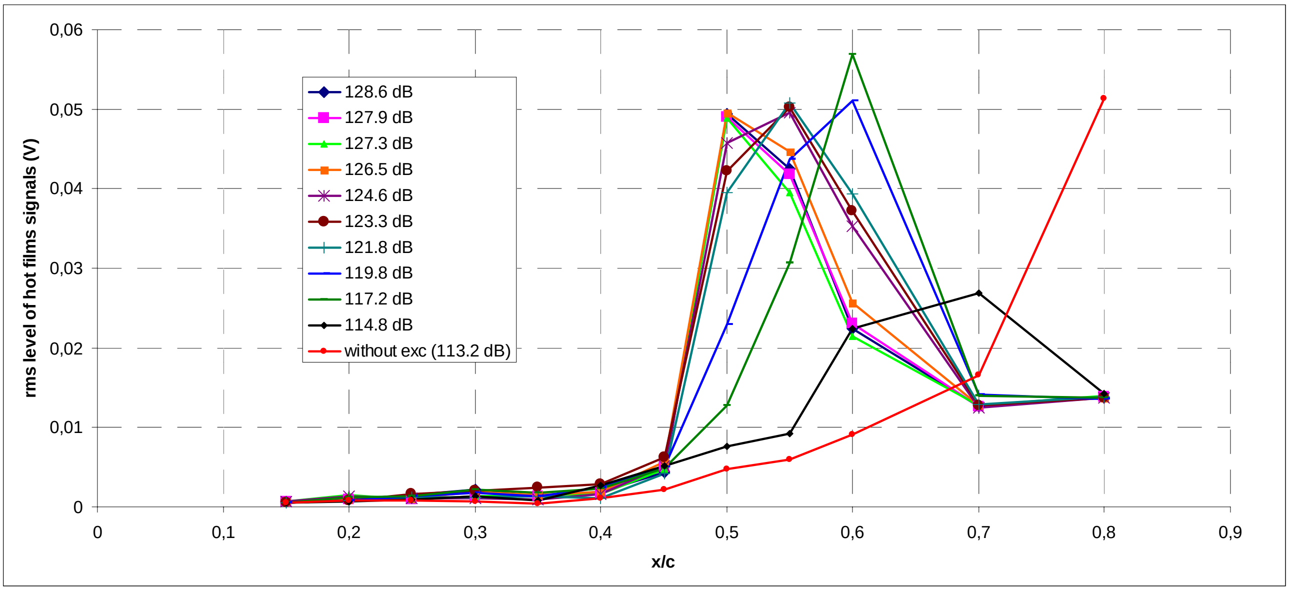

Figure 5 : Evolution of rms level of hot films versus sound level in streamwise case. Excited frequencies 2100-2300 Hz.

5 Effect of sound level on transition location

In a previous study [6], we have shown that the sound has an effect on transition location in both cases : we excite the flow with a frequency window $\Delta f = 200$ Hz sweeping between 300 and 3000 Hz for a constant sound level 120 dB. The most efficient frequency range is 2100-2300 Hz for streamwise case and 2300-2500 Hz for crossflow one. These are centered on the middle of the natural frequency range of unstable waves and are in agreement with linear stability theory. We call these frequency ranges *efficient excitation* and we choose other frequency ranges to play the role *of inefficient excitation* (1100-1300 Hz and 1300-1500 Hz, respectively for streamwise and crossflow case). In the configuration generating streamwise instabilities, we have measured an upstream shift of the transition location close to 25% of the length chord ($x_t / c = 0.45$ with efficient excitation instead of 0.7 without excitation). In the crossflow case, the same sound level produce a transition motion of only 5% chord ($x_t / c = 0.2$ with efficient excitation instead of 0.25 without excitation).

Now, we study the effect of the sound level on transition location for efficient excitation : figure 5 presents the rms level of hot films signals versus the sound level in the frequency range 2100-2300 Hz for the streamwise case. When the sound level increases, the initial progressive grow-up of the rms level is more and more bypassed and the end of transition is reached earlier. The transition length is shortened. The same result is obtained for the crossflow case (frequency range 2300-2500 Hz).

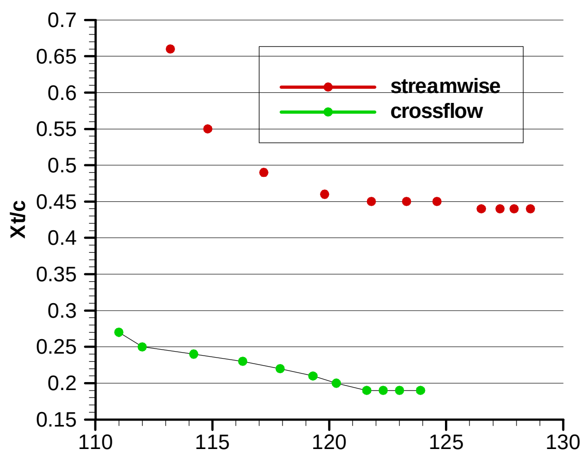

Figure 6 : Transition location evolution versus sound level.

Using the transition criterion described in § 2, we determine the transition location x_t versus sound level for both configurations as plotted in figure 6. It is important to notice that, even if a saturation of the sound effect on transition location is visible in both cases, hot films rms levels continue to move slowly versus sound level (see fig. 5). It means that using some hot films spaced each other 5% of length chord is not well-adapted to determine weak shifts of transition location.

Nevertheless, it is interesting to remark that our results about crossflow case is different from previous studies [4, 5]. Two reasons are possible:

- their transition is only driven by stationary instabilities and the acoustic excitation of travelling instabilities can not go beyond them,
- their acoustic source is not optimized (distance between source and wing, sound level or direction propagation of waves…)

In a next future, we plan to study the effect of the source location and of the direction of propagation to try to explain this difference.

6 Spectral analysis of hot films signals

The spectral analysis of instantaneous hot films signals enables us to identify the mechanisms of contribution of the excitation. The spectral method does not differentiate the spectral part due to acoustic excitation and the one due to instabilities, it superimposes them. Nevertheless, considering that the acoustic contribution is constant in the streamwise direction, we can estimate the streamwise amplification rate of instabilities (see § 8) to compare it with theory. The spectral analysis also informs us about the section as far as an acoustic wave at frequency f excites an instability wave at the same frequency.

Figure 7, relative to results at $x/c = 0.4$, illustrates two facts :

- as the sound level is identical for efficient and inefficient case, the difference of rms level in spectrum between these cases is due to instabilities amplification,
- instabilities excited by sound have frequencies confined in the excited frequency range.

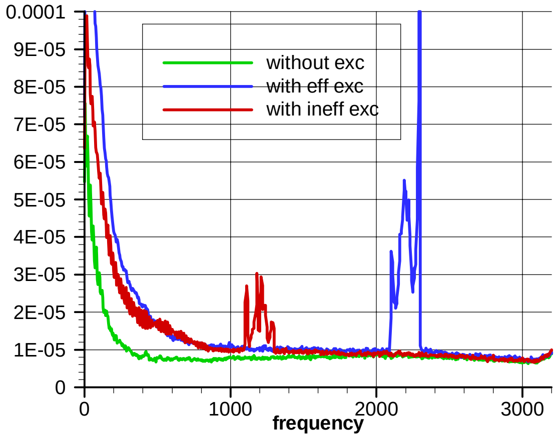

Figure 7 : spectrum of hot film signal at $x/c = 0.4$ (rms Volt)

Further downstream, at $x/c = 0.45$ (fig. 8), for the efficient excitation, some non-linear effects appear characterized by transfer of energy to neighboring frequencies and a strong deformation of spectral content of the boundary layer. It is the beginning of the transition ($x_t/c = 0.45$). It is interesting to also remark in figure 8 that in non excited or inefficiently excited cases, natural instabilities are not yet visible in spectra.

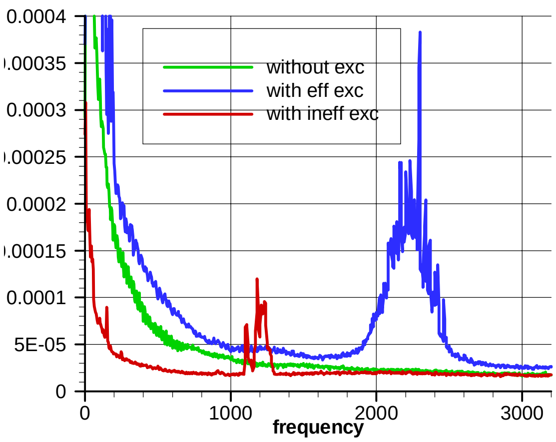

Figure 8 : spectrum of hot film signal at $x/c = 0.45$ (rms Volt).

7 Effect of sound on velocity profiles

To better understand how the acoustic excitation acts on the transition process, we compare mean and rms velocity profiles in the boundary layer with efficient, with inefficient and without excitation. Figures 9 and 10 show respectively mean and rms velocity profiles in the streamwise case at $x/c = 0.55$ (figures 11 and 12 at $x/c = 0.65$). The level of acoustic excitation is 120 dB. We present this comparison for only one case but the scenario is the same in both cases.

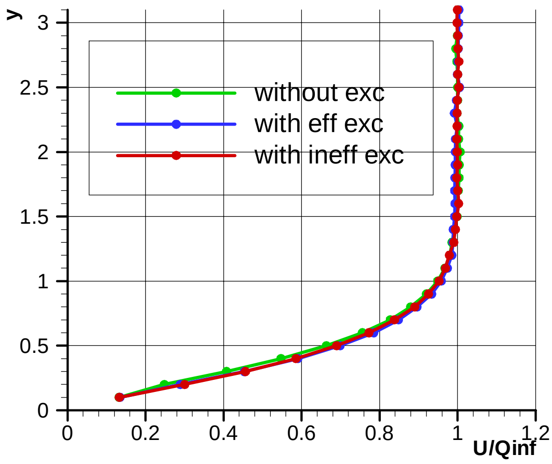

Figure 9 : Effect of excitation on mean velocity profiles at $x/c = 0.55$.

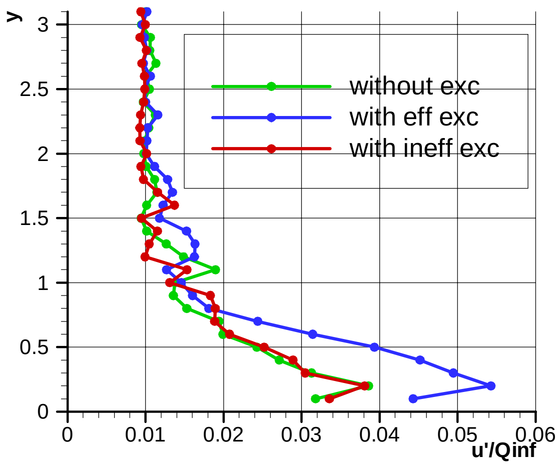

Figure 10 : Effect of excitation on rms velocity profiles at $x/c = 0.55$.

These profiles illustrate well how the efficient excitation supplies the boundary layer with energy but does not modify the shape factor ($x/c = 0.55$). We recall that, at this section, hot films indicate that the transition has already begun and that non-linear interactions exist. Downstream ($x/c = 0.65$), the boundary layer abruptly changes towards a turbulent state. The transition process is identical but it takes place on a shorter length than in the natural case. On the other hand, the effect of inefficient excitation stays invisible in boundary layer profiles.

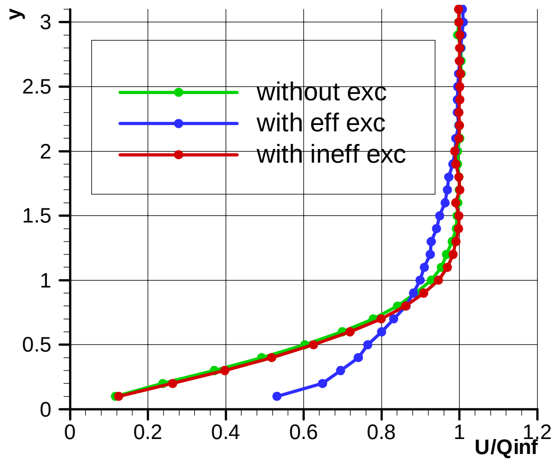

Figure 11 : Effect of excitation on mean velocity profiles at $x/c = 0.65$.

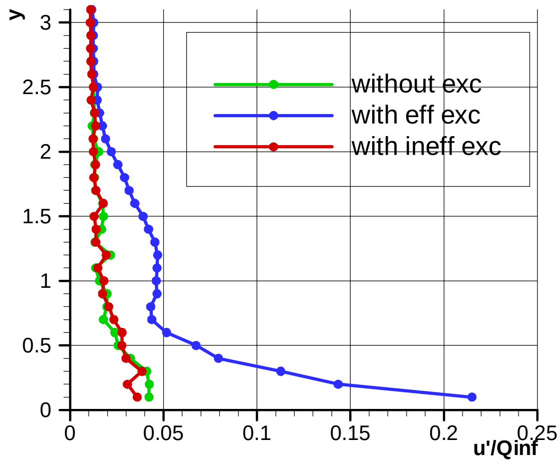

Figure 12 : Effect of excitation on rms velocity profiles at $x/c = 0.65$.

8 Comparison with linear stability theory

Our goal is to compare the experimental amplification rate (like N factor) in the streamwise direction with the theoretical one. The experimental N factor is deduced from hot film signals spectra. Figure 13 presents the evolution of these experimental N factors which are compared with the theoretical N factor computed with the fixed β^* strategy.

$A(x)$ is the rms level on spectra in the excited frequency range. So, in excited cases, this rms level includes the acoustic and instability contribution. The initial amplitudes A_0 are arbitrary chosen as all N factors are close to each other and to the theoretical one in the first sections. The absolute values of A_0 have no signification. On the other hand, the relative values of A_0 versus the excitation level are directly relative to receptivity linearity. Actually, in figure 14, we see that the initial amplitude is linearly proportional to sound level in Pascal units.

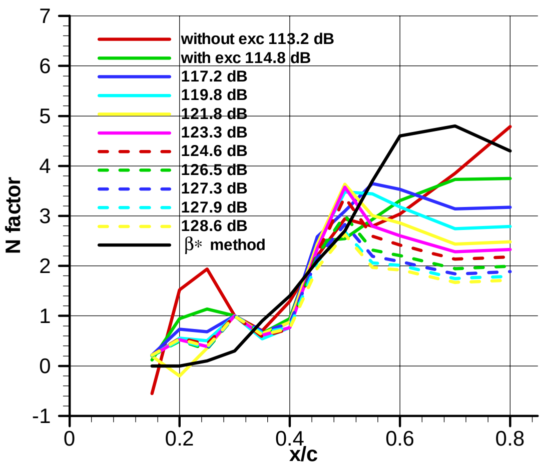

Figure 13 : N factor evolution versus sound level for streamwise case.

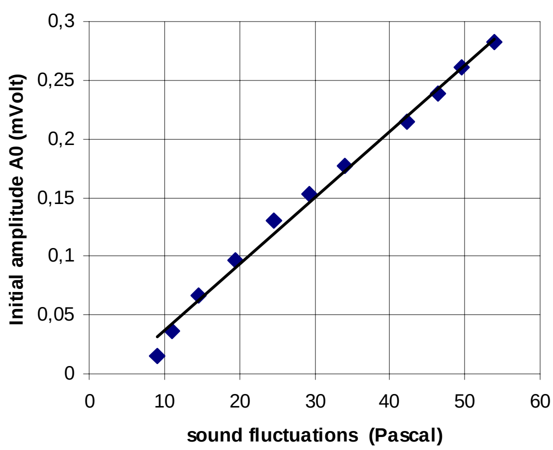

Figure 14 : Experimental initial amplitudes A_0 evolution versus sound level.

Moreover, the figure 13 proves that the experimental slopes of the N factors depend neither of the excitation presence nor its level. The sound acts as an amplifier of initial amplitude but does not modify the amplification process. The curves are different from each others at last sections because transition is reached at distinct locations. Nevertheless, it always exists a part of curves which is close to theoretical one. In streamwise case, experiments and theory diverge for $x/c \geq 0.5$. We can assume that it is due to non-linear effects which are visible on spectra from $x/c = 0.45$ (see § 6). Same investigations performed on crossflow case seem to have same conclusion but it needs some additional measurements yet.

9 N loss versus the excitation level

In practice, the interest of this kind of study is to define whether we could predict the new transition location (or its associated N factor) when an efficient excitation is performed. From the present results, we can define a relationship which links the loss of N factor at transition versus the efficient excitation level. We present in figure 15, for both configurations, the difference ΔN between N factor at transition with efficient excitation and without excitation versus the excitation level. The N values are deduced from the fixed β^* method.

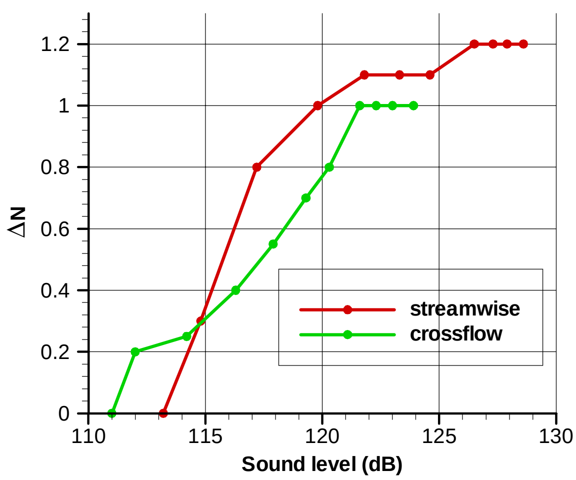

Figure 15 : ΔN evolution versus sound level.

It seems that the same level of efficient sound leads to the same loss of N factor. Even if the upstream shift of transition location is higher for streamwise case than for crossflow one (22 % instead of 6%), its lower slope of the N factor curve offsets it :

$$\frac{\partial N}{\partial x}_{streamwise} \leq \frac{\partial N}{\partial x}_{crossflow}$$

10 Conclusion

This experimental study allowed us to qualify the effect of sound on two cases of 3D boundary layer transition on swept wing. The first one is characterized by a transition due to travelling streamwise instabilities, located in a positive gradient pressure gradient area. It is close to 2D configuration with Tollmien-Schlichting instabilities. The second one is characterized by crossflow instabilities, in a negative pressure gradient. These crossflow instabilities include travelling waves and stationary longitudinal vortices. In this case, we want to check if the acoustic excitation, which acts only on travelling waves, sufficiently modifies the proportion between travelling and stationary instabilities to shift upstream the transition location.

In both cases, we showed that the transition location shifts upstream when the acoustic excitation is performed in frequency ranges of natural unstable waves (deduced from linear stability theory and checked with experiments). For the most efficient frequency ranges, we measured an upstream motion around 25% of length chord for streamwise case and only 5% for crossflow one. Moreover, we observe that the transition length is hardly shortened.

We could quantify the streamwise amplifications of instabilities versus sound intensity and to compare them with linear stability theory. It seems that the amplification factor does not depend on sound level, but the initial amplitude of instability is different. Then, this amplification factor is in good agreement with theory as far as non-linear effects are negligible.

Finally, we can propose a relationship between the loss of amplification factor (N factor) and the sound level valuable for our both streamwise and crossflow configurations. This result allows us finally to take into account the presence of measured added sound level to correct the N factor for the transition location prediction. This result is not a general criterion but only a correlation for present data.

References

[1] A.S.W. Thomas and S.G. Lekoudis. Sound and Tollmien-Schlichting waves in a Blasius boundary layer. *Research notes of Phys. Fluids* **21**(11), November 1978.

[2] W.S. Saric, E.B. White and H.L. Reed. Boundary layer receptivity to freestream disturbances and its role in transition. *AIAA* 99-3788.

[3] W.S. Saric, E.B. White. Influence of high amplitude noise on boundary layer transition to turbulence. *AIAA* 98-2645.

[4] R.H. Radeztsky, M.S. Reibert, W.S. Saric and S. Takagi. Effect on micro-sized roughness on transition in swept-wing flows. *AIAA* 93-0076

[5] H. Deyle and H. Bippes. Disturbance growth in an unstable three-dimensional boundary layer and its dependence on environmental conditions. *J. Fluid Mech*. (1996), vol. 316, pp. 73-113.

[6] S. Aubrun, A. Seraudie, D. Biron and D. Arnal. Influence of acoustic excitation on 3D boundary layer instabilities. *CEAS/DragNet European Drag Reduction Conference*. 19-21 June 2000, Potsdam, Germany.

[7] D. Arnal. Boundary layer transition : predictions based on linear theory. Presented at an *AGARD-VKI Special Course on 'Progress in transition modelling'*. March-April 1993.

Acknowledgements

This work has been supported by the "Service des Programmes aéronautiques" (SPAé).